frontiers in Physics

REVIEW
published: 20 October 2021
doi: 10.3389/fphy.2021.743316

High-Latitude Cold Ion Outflow Inferred From the Cluster Wake Observations in the Magnetotail Lobes and the Polar Cap Region

Kun Li[1], Mats André[2], Anders Eriksson[2], Yong Wei[3], Jun Cui[1] and Stein Haaland[4,5]*

[1]Planetary Environmental and Astrobiological Research Laboratory (PEARL), School of Atmospheric Sciences, Sun Yat-sen University, Zhuhai, China, [2]Swedish Institute of Space Physics, Uppsala, Sweden, [3]Institute of Geology and Geophysics, Chinese Academy of Sciences, Beijing, China, [4]Max Planck Institute for Solar System Research, Göttingen, Germany, [5]Birkeland Centre for Space Science, University of Bergen, Bergen, Norway

Cold ions with low (a few eV) thermal energies and also often low bulk drift energies, dominate the ion population in the Earth's magnetosphere. These ions mainly originate from the ionosphere. Here we concentrate on cold ions in the high latitude polar regions, where magnetic field lines are open and connected to the magnetotail. Outflow from the ionosphere can modify the dynamics of the magnetosphere. *In-situ* observations of low energy ions are challenging. In the low-density polar regions the equivalent spacecraft potential is often large compared to cold ion energies and the ions cannot reach the spacecraft. Rather, a supersonic ion flow creates an enhanced wake. The local electric field associated with this wake can be used to detect the drifting cold ions, and this wake technique can be used for statistical studies. In this paper, we review some of the key results obtained from this technique. These results help us to understand how cold ionospheric outflow varies with various conditions of solar activities and the Earth's intrinsic magnetic field.

Keywords: cold ion, ionospheric outflow, polar wind, solar wind, geomagnetic field

OPEN ACCESS

Edited by:
Gian Luca Delzanno, Los Alamos National Laboratory (DOE), United States

Reviewed by:
William Lotko, National Center for Atmospheric Research (UCAR), United States
Christopher Cully, University of Calgary, Canada

****Correspondence:***
Kun Li
likun37@mail.sysu.edu.cn

Specialty section:
This article was submitted to Space Physics, a section of the journal Frontiers in Physics

Received: *18 July 2021*
Accepted: *30 September 2021*
Published: *20 October 2021*

Citation:
Li K, André M, Eriksson A, Wei Y, Cui J and Haaland S (2021) High-Latitude Cold Ion Outflow Inferred From the Cluster Wake Observations in the Magnetotail Lobes and the Polar Cap Region. Front. Phys. 9:743316. doi: 10.3389/fphy.2021.743316

INTRODUCTION

Ions of ionospheric origin have for decades been suggested to be a very important part of the magnetospheric plasma population [1–5]. The outflow comes from both high and low latitudes, both providing significant contributions of similar order of magnitude (e.g. 106). Recent review papers summarize several studies of ionospheric outflow (107; [6–9]). Here we concentrate on the outflow from high latitudes. In terms of source region, there are broadly three regions in the high latitude ionosphere relevant for outflow and supply of ionospheric plasma to the magnetosphere. They are the dayside cusp region, the polar cap and the auroral zone.

The auroral region constitutes the boundary between open and close field lines, and is home to multiple energization mechanisms, including particle precipitation, Joule heating, quasi-static electric fields, and wave-particle interactions (see, e.g. [10,11]). Ion escaping from the auroral region can have energies ranging from a few eV to a few tens of keV. During the geomagnetic storm times, ion outflow from the auroral region contains a significant fraction of oxygen ions. A similar outflow of oxygen ions also takes place at the cusp region, where the magnetosheath has direct access to the small region of the polar ionosphere. Energization processes are similar to those in the

nightside auroral region. Due to plasma transport, outflow from the dayside cusp can also be observed over the polar cap, the high-latitude mantle, and the distant tail regions [12–16].

Poleward of the auroral region, in the polar cap, magnetic field lines are "open" (connected to the interplanetary magnetic field). Upflow in this region is initially driven by an ambipolar electric field set up by the difference in scale height between electrons and ions. Simulations (e.g. [17]) and observations (e.g. [18]) suggest a total potential drop of a few volts due to this ambipolar electric field. Energization is thus only a few eV, but this is enough to energize light ions sufficiently to escape Earth's gravitational field. Low-energy ionospheric outflow set up by this ambipolar electric field was firstly predicted by Axford [19] and Banks and Holzer [20], and is often referred to as the polar wind. Additional acceleration mechanisms such as the mirror force and the centrifugal force [21,22], provide some additional energy, but these ions typically remain "cold" for a long time as they move through the magnetosphere.

On short time scales, ouflow of these cold ions plays an important role for dynamics of the magnetosphere (e.g. [23]). Due to the combination of parallel motion along the magnetic field lines, and perpendicular motion through convection of magnetic flux tubes, a large fraction of ions emanating from the ionosphere end up in the Earth's tail plasma sheet after having been transported through the magnetospheric tail lobes. The nightside plasma sheet is of key importance for magnetospheric dynamics and space weather effects like geomagnetic storms and substorms. In particular, magnetic reconnection taking place in the thin current sheet, converts magnetic energy to kinetic energy and results in the deposition of large amounts of energy into the inner magnetosphere, the ring current and the auroral ionosphere.

On a microscopic scale, magnetic reconnection implies a decoupling between particles and the magnetic field in a localized region. This leads to the creation of an electron diffusion region and an ion diffusion region, which scale sizes are governed by the respective inertial lengths and gyroradii of the ions and electrons. Due to their low energy and temperature compared to the pre-existing ions in the plasma sheet, cold ions effectively introduce an intermediate diffusion region into this picture [24,25]. The kinetic physics of reconnection can be drastically changed when cold ions are introduced, e.g., by locally reducing the Hall currents and by introducing new instabilities [26–28]. The large-scale reconnection rate does not seem to change much, at least not for magnetospheric conditions [29].

On geological time scales, ionospheric outflow can also influence the evolution of the atmosphere [30–33]. A frequently recurring question here is the role of a planet's intrinsic magnetic field. On one side, it is claimed that a magnetic field provides some protection against direct solar wind interaction (e.g. [34]), but on the other side, and as noted above, a magnetic field also facilitates some of the escape mechanisms responsible for long term atmospheric evolution (e.g., [35,36]) [37]).

Measuring low energy ions in the terrestrial magnetosphere is notoriously difficult. In the Earth's low density magnetotail lobes, spacecraft are usually positively charged due to photoelectron emission. This positive electric potential effectively shields the spacecraft and its instruments from any ions with energies lower than the equivalent electric potential energy of the spacecraft. Consequently, direct measurements of cold ions with particle detectors in this part of the magnetosphere are not possible unless the spacecraft charge can be neutralized [1,3,4,9,38]. Cold ions in the magnetosphere have therefore been considered "invisible" for a long time. However, an indirect method, based on observations of an enhanced electrostatic wake by the Cluster satellites made it possible to determine the bulk flow velocity of cold ions [39–41]. In this paper, we briefly review this wake method and some of the key results obtained from this technique.

This paper is organized as follows: In *Detecting Cold Ion Outflow*, we first outline the methodology to infer flow velocity and density of cold ions from Cluster mission data, and then briefly introduce the observations of ionospheric outflow prior to the Cluster mission. In *Transport of Cold Ions in the Magnetosphere*, we present results based on a large data set of wake measurement from the Cluster satellites. In particular, we use these observations to infer the ionospheric source region, transport paths and fate of the outflowing ions. In *The Role of the Earth's Intrinsic Magnetic Field* and *Energy Sources for the Outflow*, we present studies on the role of the Earth's magnetic field and the energy sources of cold ion outflow, respectively. In Discussion, we discuss possible comparison using results from the wake technique on Earth with observational studies for other terrestrial planets. Finally, *Summary* summarizes the paper.

DETECTING COLD ION OUTFLOW

Characterization of cold ion outflow requires knowledge about number density and flow velocity of the cold ions. A major challenge with *in-situ* spacecraft observations of low energy plasma is spacecraft charging. One primary source region, the polar cap, is magnetically connected to the magnetospheric lobes—large regions of space characterized by very low plasma densities, typically less than 0.1 cm^{-3} (e.g. [42]). A sunlit spacecraft in such environments will rapidly be charged up to several tens of volt due to photoemission of electrons (e.g. [43,44]). This spacecraft charging acts as a barrier to ions with energies below energy associated with the electric potential of the spacecraft. Consequently, cold ions will be invisible for particle detectors onboard the spacecraft, so alternative methods to determine density and flow velocity have to be used.

Cold Ion Density Determination

In addition to particle instruments and calculation of plasma moments, two alternative methods to determine cold plasma density are possible with Cluster observations. The Wave of HIgh frequency and Sounder for probing Electron density by Relaxation (WHISPER—see e.g. [45]) relies on the identification of the plasma frequency in a wave spectrum and can provide very accurate measurements of electron densities. However, it is not always possible to automatically determine a

single unique resonance line, so densities from WHISPER are not always available. Furthermore, in active mode, WHISPER operation involves excitation over a wide frequency range to determine the resonance line. The lowest possible excitation frequency of WHISPER is around 4 kHz, corresponding to approximately 0.2 cm^{-3} as the lowest detectable electron density value. In addition, contamination from the locally produced photoelectrons can also influence WHISPER measurements.

A second, and frequently used method is based on utilization of the spacecraft charging [44,46]. As shown in e.g. Pedersen et al. [46], a functional relationship between spacecraft charge and the ambient electron density of the form, $N_e = A \exp(-\frac{V_{sp}}{B})$, exists. Here, N_e is the electron density and V_{sp} is the spacecraft potential relative to the ambient plasma. On Cluster, the spacecraft potential is routinely measured by the Electric Field and Wave instrument (EFW- see [47]). A and B are empirical constants, and can be determined from cross-calibration with other instruments including the CIS [48], PEACE [49] and WHISPER [50] when densities obtained from these instruments were available (e.g., [44,46]). Assuming quasi-neutrality, the cold ion density is identical to electron density. This technique has been used by e.g. Svenes et al. [42], and Haaland et al. [51,52] to study cold ion density in the polar cap and lobe regions and their response to changes in the solar irradiation and solar wind—magnetosphere coupling.

Cold Ion Bulk Velocity Inferred From Electrostatic Wake Measurements

Spacecraft in the low-density lobes are often positively charged to tens of volts. The outflowing positive ionospheric ions are typically supersonic with bulk velocity corresponding to an energy of only a few eV and an even lower thermal velocity. These ions are not deflected by the spacecraft body but by the much larger electrostatic structure due to the spacecraft voltage, causing an enhanced ion wake. Since the flow is subsonic with respect to the thermal speed of the electrons, the wake charges negatively. Both ions and electrons can here be treated as essentially unmagnetized (e.g. [39–41,53]). Consequently, a local electrostatic electric field arises due to the wake caused by the charged spacecraft. By measuring this electric field of the wake region, as well as the unperturbed electric field outside the wake, the velocity and direction of the bulk cold ion flow can be determined [53]. Cluster, with its two complementary electric field instruments, is able to measure both the wake field and the unperturbed electric field.

Each wire boom pair of the EFW instrument has two probes 88 m apart. Given a length scale of the wake on the order of 100 m [41,54], the electric field measured by EFW, E^{EFW}, is a superposition of the wake field and large-scale background electric field.

The unperturbed electric field can be measured by the Electron Drift Instrument (EDI) [55,56]. EDI emits electron beams with an energy of 0.5 or 1 keV in the direction perpendicular to the ambient magnetic field, B. The emitted electrons gyrate and return to the instrument, where their gyro center displacement ("drift step") and thus convection are determined. In the magnetotail lobes, the gyro-radius of the emitted electron beams is usually on the order of kilometers and thus much larger than the wake dimensions. The electric field measured by EDI, E^{EDI}, is thus largely unaffected by the wake field.

The wake field can be calculated by subtracting the two measurements, $E^W = E^{EFW} - E^{EDI}$, and since the ions are essentially unmagnetized this gives the direction of the bulk flow velocity, u. In the magnetotail lobes, the perpendicular bulk velocity of cold ion flow is equal to the magnetospheric convection velocity, $u_\perp$, which can be inferred from $u_\perp = E^{EDI} \times B/B^2$. With knowledge about the direction of the total bulk flow velocity and the perpendicular convection, the parallel bulk flow velocity, $u_\vee$, of cold ions can be determined. Combined with cold ion density estimated from the spacecraft potential as described above, it is possible to calculate the flux of cold ions. Details concerning the data analysis and error estimates are given by [40] and in Appendix A of André et al. [5]. A comparison between the enhanced wakes in the polar lobes and narrow wakes in the solar wind and in low Earth orbit is given by André et al. [8].

Data Set of Cold Ions

Many studies have investigated ion outflow at high latitudes. Early observations with particle detectors on satellites include hydrogen polar wind outflow by [57] and the discovery of precipitating keV oxygen ions in the magnetosphere by [58], showing the existence of an ionospheric ion population at higher altitude. Observations have then been obtained by several satellites including S3-3, Dynamics Explorer 1, Viking, Akebono, Freja, Polar, FAST, DMSP and Cluster, by several sounding rockets, and by the European Incoherent Scatter (EISCAT) radar and the EISCAT Svalbard (ESR) radar. A schematic summary of observations is given in **Figure 2** in Yau et al. [59] and recent reviews are given by [7,60]), André et al. [8] and Toledo-Redondo et al. [9].

In the ionosphere a spacecraft can be negatively charged due to the high density and high flux of electrons. At higher altitudes in a low-density plasma, the photoelectrons emitted by a spacecraft in sunlight can dominate, causing positive charging. At altitudes of several R_E (Earth radii) in the polar lobes, spacecraft charging of tens of volts positive is common. This will obviously prohibit positive ions of ionospheric origin with energies of a few eV to reach the spacecraft.

Comparing observations of low-energy ions by different particle detectors using different techniques with different nominal lowest energy channels on different spacecraft, is not trivial. For statistical studies this must include different phases of a solar cycle in different regions, with gradually increasing spacecraft charging as altitude is increasing and density is decreasing. Nevertheless, it is clear that in the energy range where particle detectors and the wake method overlap (order 10 eV) results from low altitudes (ionosphere to a few thousand kilometers) where spacecraft charging is less of a problem and from high altitudes (several Re), both techniques give an average total outflow rate of the order 10^{26} ions s^{-1}, see Table 2 in Peterson et al. [61], Table 1, André et al. [8] and Table 2, Toledo-Redondo et al. [9].

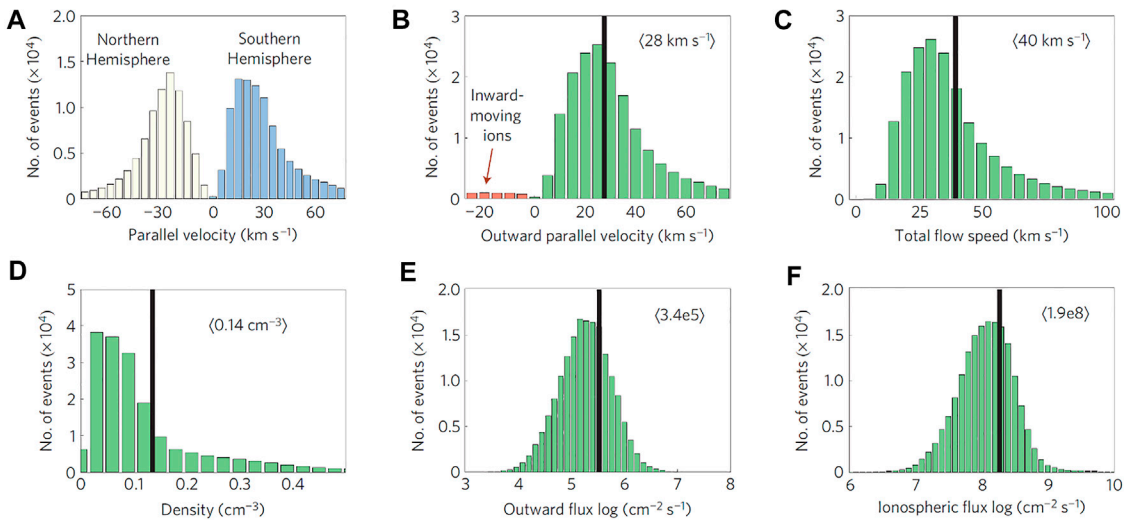

FIGURE 1 | Properties of cold ion outflow. **(A)** Parallel velocity. **(B)** Outward velocity aligned with the magnetic field lines. **(C)** Total speed of cold ions. **(D)** Cold ion density derived from measurements of spacecraft potential. **(E)** Outflow flux calculated from outflow parallel velocity times density with a fact of 0.8 for proton, assuming the outflow consists of 80% of protons. **(F)** Flux in the topside ionosphere mapped from the locations of Cluster to the altitude of 1000 km, where the strength of the magnetic field is assumed to be 37 μT. Adopted from [53].

The spacecraft potential at high altitude can during some periods be artificially reduced by emitting a plasma cloud (the Polar satellite [3]) or a beam of positive ions (Cluster and MMS, [62,63]). Typically a satellite potential of a few volts positive remains. Observations by the Polar satellite at altitudes of 5,000 and 50,000 km using active spacecraft potential control and particle detectors are roughly consistent with the Cluster observations we discuss in detail, although a significant fraction of the low-energy ions may still not reach Polar ([3,40,53,61,64,65]. *In situ* comparison of two Cluster spacecraft in the same polar lobe region at an altitude of about 100,000 km give similar results for both satellites, with one spacecraft using the wake method and the other using particle detectors and artificial reduction of the spacecraft potential [39]. Again direct detection of ions with an onboard instrument, and the Cluster wake technique, give consistent results. The techniques have different advantages. For example, a mass spectrometer can identify different ion species, while the wake technique can detect ions down to the lowest thermal energies and can routinely be used for statistical studies covering many years.

Detailed comparison is further complicated by the fact that ions typically are gradually energized as they move upward. Particle tracing over altitude ranges of several R_E using different observations to initiate the particles still give reasonably consistent results. Tracing based on observations by Polar [66], Akebono [67,68] and on the Cluster wake method [69,70] all show that low-energy ions are common in the magnetotail lobes and often are a significant supply to the tail magnetosheet.

The Cluster wake technique can detect low energy (eV) positive ions also using instruments on a spacecraft charged to tens of volts positive, and can be used for statistical studies during many years. As described above, this technique is based on supersonic flowing ions causing an enhanced wake. Using this technique, and 5 years of observations from one of the four Cluster satellites, ([39,53] presented the first survey of cold ion measurements in the polar cap and lobe regions. Their results demonstrated that the ionospheric outflow during most of the time is dominated by very cold ions—a population that until then had been invisible. By combining outflow velocity and density [40], also estimated the total outflow rate to be the order of 10^{26} ions s^{-1}. As noted above, this value is consistent with observations at much lower altitude where spacecraft charging is less of a problem, but is higher than that in previous studies at high altitudes based on measurements of ions with higher energies (Table 1), [53].

The outflow velocities derived from the wake method, the simultaneously obtained outflow density from spacecraft potential measurements, and outflow fluxes are summarized in **Figure 1**. **Figure 1A** is the histogram of the parallel velocities of cold ions. The mean parallel velocity of outward moving cold ions is 28 km s^{-1}. There are also a few cases of inward moving cold ions as seen in **Figure 1B**.

A follow-up study using the wake technique was presented by André et al. [5]. They used measurements from two of the four Cluster satellites over a 10-year period (2001–2010, nearly a full solar cycle). During this time EDI was operational on the two spacecraft, so velocity estimates could be obtained, needed to estimate the flux. For each year data from 3 July to 3 November were used, centered on 3 September when the polar orbit apogee of about 20 R_E was at local midnight and thus close to the center of the geomagnetic tail behind the Earth, although this time period may introduce a hemispherical seasonal bias because it is closer to the northern summer solstice than to the southern summer solstice. All parts of orbits on the nightside ($X_{GSM} < 0$)

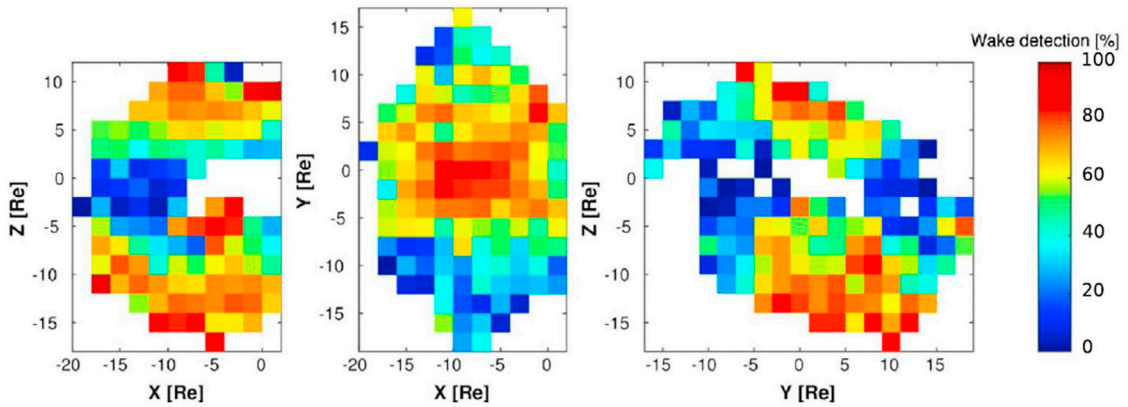

FIGURE 2 | The occurrence rate of cold ions defined by wake detection. A total of about 1,680,000 data are obtained from Cluster 1 and 3 during the years from 2001 to 2010. Adopted from [5].

and geocentric distances beyond 5 R_E were used. In this study, approximately 1,680,000 data points (4 s spacecraft spins) were used to search for enhanced wakes. The presence of a wake was detected in approximately 1,070,000 data points, corresponding to 64% of the total observation time. Cold ions are therefore present in the lobes and polar cap regions most of the time. **Figure 2** shows the occurrence rate of cold ions inferred from wake detections as color-coded maps. The occurrence rate is defined as the ratio of number of wake detections to the total number of measurements in the spatial ranges of the grids in **Figure 2**. In many regions, the occurrence rates of wake detection were above 50%.

After selection of data points with low enough error to be used for estimates of density, velocity, and flux, the number of data points is reduced to 320,000. These data show that the outflow of cold ions is of the order of 10^{26} ions/s and often dominates over the outflow at higher energies.

In addition to the pioneering studies by [39,40] and André et al. [5], a number of other studies (e.g. [69–76]) have made use of this data set to investigate the role of cold ions in the magnetosphere. *Transport of Cold Ions in the Magnetosphere* and *The Role of the Earth's Intrinsic Magnetic Field* of our paper discuss some of the key results from these studies.

TRANSPORT OF COLD IONS IN THE MAGNETOSPHERE

Transport of cold ions from their source in the high latitude polar ionosphere is facilitated by a combination of parallel motion of the ions along the magnetic field, and the convection of magnetic flux tubes due to the solar wind-magnetosphere interaction.

Since the Cluster observations are obtained from point measurements of E-fields, mainly in the high-altitude polar cap and lobe regions, they do not provide much information about the transport paths of ions. Neither the source region nor the fate of the outflowing ions can be directly determined from local measurements alone. One possibility to assess details about the transport of cold ions through the magnetosphere is to use particle tracing. Using a model of the Earth's magnetic field, and the observed convection at Cluster [69,70], used first order guiding center approximations [77] to trace the motion of individual ions from the location of Cluster, either backward to the source region of the ions in the ionosphere, or downtail to the Earth's plasma sheet where many cold ions end up.

Mapping the Ionospheric Source of Cold Ions

One of the objectives of the Li et al. [69] study was to assess the role of solar wind-magnetopshere interaction and geomagnetic activity on ion outflow. **Figure 3**, adapted from their paper, shows color coded maps of source regions of the cold ions for various geomagnetic disturbance activities as reflected by the Dst index. The fluxes shown in the figure are mapped to the altitude of 1000 km. The upper row shows maps for the northern hemisphere and the lower row shows maps for the southern hemisphere. From **Figure 3**, one notes that geomagnetic activity influences cold ion outflow and the source regions in two ways. The outflow flux varies, and the source area changes with geomagnetic activity.

During quiet conditions (Dst>0 nT, shown in panels 1) and 4)), the outflow fluxes are fairly low, on the order of 10^8 ions s^{-1} cm^{-2}, and mostly emanating from a rather small area at high latitudes in the polar cap. Conversely, during high activity (Dst < -20nT, panels 3) and 6)), outflow fluxes are higher by almost an order of magnitude, and the outflow now occurs from a larger area. This is consistent with and expanding/contracting polar cap during disturbed/quiet conditions (e.g. [78]).

The increased flux during disturbed conditions can probably be attributed to a combination of enhanced ionization (e.g. [5]) and enhanced upward/outward forces such as the mirror force or centrifugal force [21,22,79].

From **Figure 3**, it is also seen that there are regions of enhanced outflow near the dayside cusp and the nightside auroral region during disturbed conditions. This may suggest

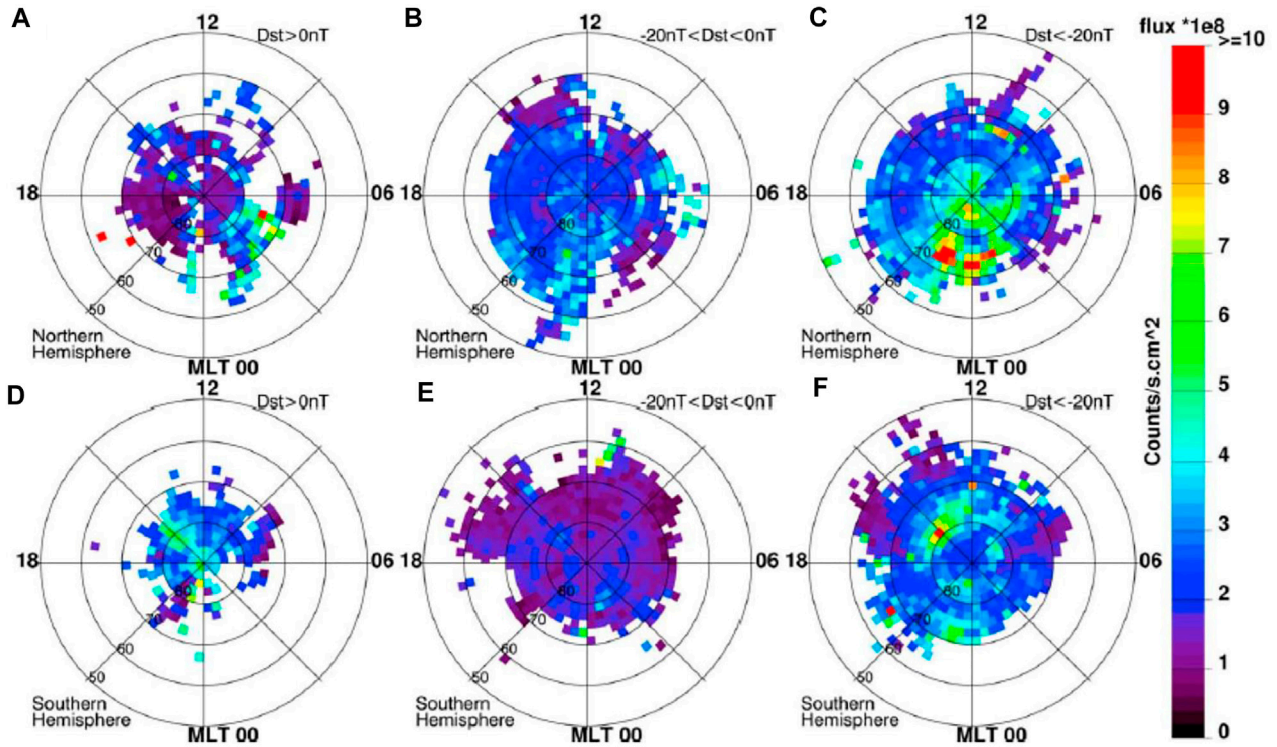

FIGURE 3 | Cold ion outflow flux in the northern **(A–C)** and the southern **(D–F)** hemispheres. For each hemisphere, the three panels from left to right show the fluxes under quiet, moderate, and disturbed geomagnetic conditions, respectively. Each colored pixel indicates the mean flux. From Li et al., (2012).

that particle precipitation or energy flux in the form of waves from the solar wind or the magnetosphere drives some of the outflow. The apparent north-south asymmetry in outflow flux was caused by the Cluster's orbit. Due to the tailward magnetospheric convection, ions escaping from the dayside are likely to travel to higher altitudes than that from the nightside. During the time when cold ions were measured, the Cluster satellites were at higher altitudes in the southern hemisphere than in the northern hemisphere. Therefore, we see more ions from the dayside of the southern polar cap and also from the nightside of the northern polar cap.

To study changes in the cold ion outflow during different phases of geomagnetic storms, Haaland et al. [72] have divided the data from André et al. [5] into subsets according to different phases in various storm events. They have calculated the total outflow rates from the measured outflow fluxes and simultaneously estimated areas of the outflow region, which are modulated by the upstream solar wind conditions and the intensity of the ring current [78]. It is found that the outflow rates and the size of outflow regions are moderate before the main phase of a geomagnetic storm. During the storm main phase, both the cold ion density and velocity increase, and the polar cap regions expand. The average outflow rate increases by almost an order of magnitude during the peak phase of a generic storm compared with the quiet time. The increased outflow velocity may be attributed to larger centrifugal forces during the main phase with enhanced magnetospheric convection.

Determining the Fate of Cold Ions

As noted above, transport of cold ions in the magnetosphere is controlled by the combination of motion along the magnetic field and magnetospheric convection. In the stretched magnetic field of the magnetotail lobes, convection is mainly towards the central plasma sheet, and the same for all species and energies. The parallel velocity, on the other hand, is generally different for different energies of the ions. This leads to a velocity filter effect that separates ions by energy and origin.

Ions with a high parallel velocity can escape the magnetotail and be lost into the solar wind without reaching the plasma sheet, while ions with lower parallel velocities can reach the plasma sheet where they eventually get heated. Likewise, ions starting at high latitudes, or the dayside ionosphere, will have longer transport paths than ions from lower latitudes in the nightside, and are more likely to be lost (e.g., [12,14,32]).

Haaland et al. [71] used the convection velocities obtained from the Cluster/EDI measurements and parallel velocities and flux of cold ions to estimate the fate of cold ion outflow. Their results, summarized in **Figure 4**, show that the fate of outflowing ions is highly affected by the interplanetary magnetic field (IMF) and consequently the level of the geomagnetic activity. A northward IMF leads to nearly stagnant magnetospheric convection, but there is still cold ion outflow. Under such conditions, most of the outflowing cold ions are lost downtail into the solar wind. The fraction of cold ions directly lost in this way varies from about 4% during storm periods to about 96%

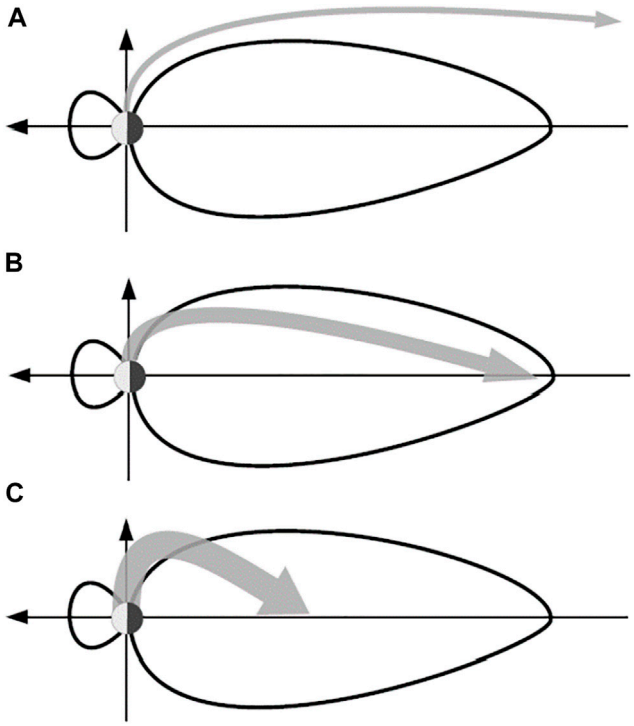

FIGURE 4 | Schematic plots of the trajectories of cold ions during **(A)** quiet, **(B)** moderate, and **(C)** storm periods. The width of the grey arrow in each panel indicates the flux of cold ions. The geomagnetic quiet conditions correspond to near stagnant magnetospheric convection, with relatively small outflow fluxes from the ionosphere. Strong magnetospheric convection happens during the geomagnetic storm periods. Although the outflow fluxes are large compared to that during the quiet periods, most of the cold ions reach the plasma sheet before moving far down-tail. From Haaland et al. [71].

during quiet periods. This is consistent with the recent results that the plasma sheet is primarily supplied by ions of ionosphere origin during storm periods [80].

Cold ions are mainly accelerated by the centrifugal force during the transport through the magnetosphere [53,81,82]. The centrifugal force is small, so that cold ions typically remain cold. Li et al. [70] used particle tracing to study the transport of cold ions in more detail. Their results showed that it takes about 2–4 h for a cold ion to travel from the ionosphere to the plasma sheet. Due to enhanced convection, and to some degree increased parallel velocity, the travel time decreases with increasing geomagnetic activity. During the geomagnetic storm periods, cold ions therefore land on the plasma sheet closer to the Earth than during the quiet periods. Furthermore, the results show a persistent dawn-dusk asymmetry with more cold ions ending up near dusk, even though there is no such asymmetry in the source region. This is consistent with simulations by Cully et al. [67] for low-energy ions and by [83] for O^+ ions. This phenomenon can be explained by the fact that the movements of outflowing ions are largely constrained by the convection electric field. The averaged convection equipotentials are skewed 2–3 h clockwise under most conditions, as simulated by Weimer [84] and observed by Haaland et al. [85]. Therefore, ions from the dayside traveling tailward typically have a velocity component in the duskward direction and end up in the dusk sector of the plasma sheet.

THE ROLE OF THE EARTH'S INTRINSIC MAGNETIC FIELD

Throughout Earth's geological history, both orientation and strength of the geomagnetic field have changed dramatically, often within short geological time scales (e.g., [33,86–88]). Changes in the magnetic field will affect the shape, size and location of the polar cap—the source region for cold ion outflow—and consequently the total outflow. Ion outflow is also affected by the strength of the geomagnetic field, since this will influence the interaction between the solar wind and the atmosphere.

In the following, we show how changes in orientation of the geomagnetic field due to the rotation of Earth impact cold ion outflow. We also show how cold ion outflow is affected by changes in strength of the geomagnetic field based on comparison studies of outflow from ionospheric source regions with different geomagnetic field strength, but with similar solar zenith angles and levels of geomagnetic activities. The results of these studies help us to understand the importance of magnetic field strength for quenching planetary mass loss.

The Impact of Geomagnetic Field Orientation

Due to the rotation of the Earth and the offset between the geomagnetic dipole axis and the rotation axis, the geomagnetic dipole tilt angle varies on a seasonal and diurnal basis. This results in corresponding variations in the illuminated area of the polar cap. Studies based on simulations (e.g. [89]) and observations (e.g. [90]) show that variations in the plasma density and temperature in the ionosphere are significantly influenced by the Solar Zenith Angle (SZA). Using the above described cold ion data derived from the plasma wake, Maes et al. [76] showed that both cold ion density and cold ion outflow velocity decrease with increasing SZA, with substantially lower plasma density and outflow velocity for SZA values larger than about 100°.

Figure 5 shows various cold ion outflow parameters in the topside ionosphere [73] as a function of solar wind energy input rate under different conditions of solar EUV and hemispheric dipole tilt angle (μ) using the cold ion data base obtained with Cluster [5]. Here, the μ is defined as the tilt angle of the projection of the outward directed dipole axis on the GSE XZ plane, it is positive or negative as the axis in the hemisphere tilts toward the Sun or the tail. The solar wind energy input rate is estimated from the ε parameter as a measure of the electromagnetic Poynting flux that enters the magnetosphere [91].

As we can see in **Figure 5**, changes in μ controls the outflow density (**Figure 5A**), and the outflow density also increases with increasing solar wind energy. In contrast, turning of μ from negative to positive seems to result in a small increase in the parallel velocity (**Figure 5B**). Comparing the values in **Figure 5C**

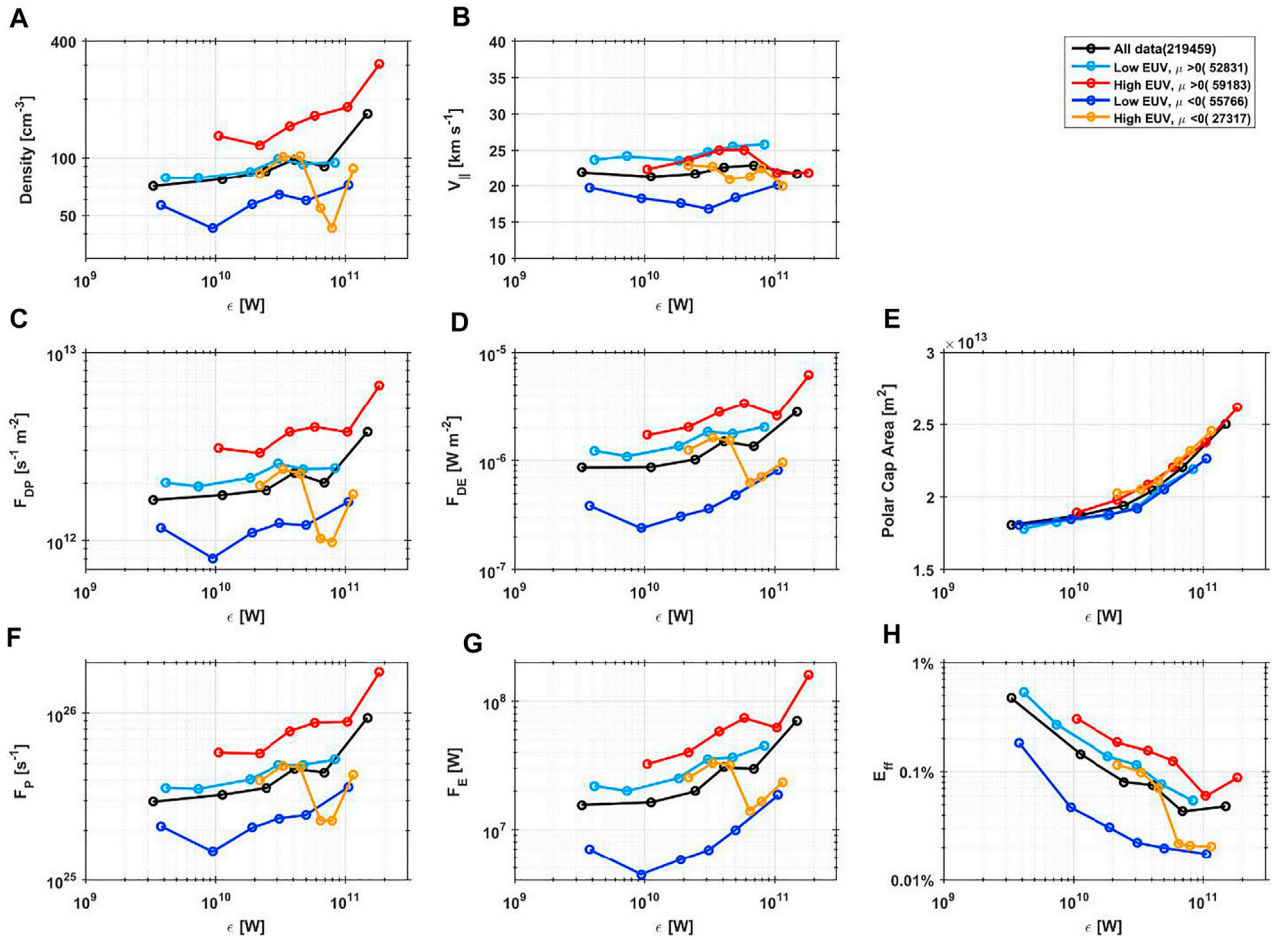

FIGURE 5 | Cold ion outflow parameters in the topside ionosphere as a function of the ε parameter under different conditions of solar EUV and geomagnetic dipole tilt angle (μ). Each panel shows median values calculated from the 10-years data set described in *Data Set of Cold Ions*. High and low solar EUV are defined as $F_{10.7}$ being higher and lower than 155, respectively. F_{DP} and F_P stand for outflow particle flux and outflow rate, respectively. F_{DE} and F_E are outflow energy flux and outflow power, respectively. E_{ff} is the energy coupling coefficient calculated from $E_{ff} = F_E/\varepsilon$. From Li et al., (2017).

with different signs of μ but with the same ε parameter under the condition of high solar EUV, the increases in the density and the velocity result in an increase in the outflow particle flux (F_{DP}) and the outflow energy flux (F_{DE}) by a factor of 2 as μ turns from negative to positive. The condition of high solar EUV and negative μ cannot be used for comparison because the number of data points under this condition is not comparable to that under other conditions. The turning of the dipole axis does not change the polar cap area. So, the total hemispheric outflow rate of particle (F_P, shown in **Figure 5F**) and total hemispheric outflow rate of energy (F_E, shown in **Figure 5G**), respectively calculated from F_{DP} and F_{DE} times the outflow area (**Figure 5E**, see details of calculation in [73]), also increase by a factor of 2 as μ turns from negative to positive.

Therefore, the geomagnetic orientation can control the F_P and the F_E by changing the outflow density. The changes in the parallel velocity due to changes in the geomagnetic orientation is considerably small and can be statistically negligible in estimating the F_P and the F_E.

The Impact of Geomagnetic Field Strength

In addition to variations over time, the geomagnetic field also possess strong spatial inhomogeneities (e.g., [92]; 109). In particular, and perhaps best known, the region of reduced field strength known as the South Atlantic Anomaly (e.g., [93]; 108 [94]) allows particles to penetrate deeper into the atmosphere due to the lower mirror altitude, and can locally modify the ionosphere (e.g., [93,95,96]). More relevant for ionospheric outflow is the magnetic field strength in the polar cap regions [97].

Li et al [75] investigated the role of geomagnetic field strength in ion outflow. They analyzed the outflow from different regions of the polar cap ionosphere in the southern hemisphere where there are significant spatial inhomogeneities in magnetic field strength. The northern polar cap has a relatively uniform spatial distribution of magnetic field [97] and thus the data from the northern hemisphere are not used for the analysis. Once again using the above described Cluster wake data set and particle tracing, they determined the outflow density (n) and the outflow

particle flux (*Fp*) at the locations of the source region. The magnetic field strength in the source region of the outflow, $|B|$, is obtained from the international geomagnetic reference field (IGRF) model. They sorted the observations into subsets according to levels of geomagnetic activity (AE index), solar activity ($F_{10.7}$), and SZA.

The results shown in **Figures 1–3** of Li et al. [75] suggest that there is an anti-correlation between $|B|$ and n (and F_P as well). Their results suggest that the anti-correlation mostly happen during periods with the $F_{10.7}$ index between 150 sfu and 200 sfu. When $F_{10.7}$ was either smaller than 150 sfu or larger than 200 sfu, the anti-correlation became less prominent. This can be explained by the contraction and inflation of the atmosphere during low and extremely high solar activities. Let us assume that electrons precipitate from the lobes or solar wind with the same properties (such as pitch angle, energy, density, and strength of magnetic field at their source region) for outflow events in similar levels of geomagnetic activity with similar SZAs. In the case of low solar activities, the precipitating electron cannot reach the atmosphere. In the lcase of extremely high solar activity, all energies of the precipitating electrons will be lost in the atmosphere. This leads to the fact that the occurrence rate of anti-correlation is low when the level of solar activity is low or extremely high. Therefore, within the range of the magnetic field strength in the polar region of the southern hemisphere at present time, the intrinsic magnetic field is anti-correlated with ionospheric outflow during the periods of high levels of solar activity (150 sfu < $F_{10.7}$ < 200 sfu).

Energy Sources for the Outflow

To estimate how efficiently the Sun transfers energies to ion outflow, the power of ion outflow (defined in *The Role of the Earth's Intrinsic Magnetic Field*, as the hemispheric outflow rate of kinetic energy carried by escaping cold ions) stemming from solar wind and solar illumination are quantified. These quantities are important to answer the question (though this question is highly debated and remains open): whether the intrinsic magnetic field of a planet is necessary to prevent loss of its atmosphere into space?

Li et al. [73,74] investigated how efficiently solar energy in the form of illumination and Poynting flux, is converted to energy driving ionospheric outflow at Earth. A proxy for solar energy input rate was derived from measurements of the solar wind (the ε parameter—see e.g. [91]), and solar illumination (calculated from the total solar irradiance (TSI) of 1,361 W m^{-2} [98], which is the solar electromagnetic irradiation power per unit area integrated over all wavelength, times the cross-sectional area of the ionosphere looking from the Sun). The above-described cold ion data set based on Cluster wake measurements, combined with a total outflow area as based on an expanding/contracting polar cap as described in [78] were used to estimate the total power of ion outflow.

Figure 6 shows how the total hemispheric power of the outflowing ions, F_E, varies as a function of the solar wind energy input rate. **Figure 6A** shows the results for an illuminated polar cap source region, and **Figure 6B** shows the corresponding results for a dark polar cap region. These results indicate that solar wind energy is the main energy source for the cold ion outflow when the ε parameter is larger than 10^{10} W.

When more than 95% of the polar cap is illuminated (**Figure 6A**), the total hemispheric power associated with the outflow of cold ions increases from 10^7 W to 10^8 W with increasing solar wind energy input. However, when the ε parameter is smaller than 10^{10} W, the outflow power, F_E, is almost a constant around 10^7 W when the polar cap is illuminated, suggesting that solar illumination rather than solar wind energy input in the form of Poynting flux, is the primary energy source for the outflow.

For dark conditions (**Figure 6B**), F_E is almost an order of magnitude smaller. From this, Li et al [73,74] inferred that solar illumination alone provides energy sufficient to sustain outflow power of the order of 10^7 W, indicating that the main energy source for cold ion outflow is the solar illumination when the ε parameter is smaller than 10^{10} W.

We note that F_E is not zero when the combined solar wind Poynting flux and solar illumination are extremely small. This may be explained by transport of energy from the illuminated area outside the polar cap due to the circulation in the atmosphere. Polar rain precipitation or more energetic precipitation inside nightside polar cap region may also contribute to energization.

From **Figure 5H**, we also infer that only about 0.1% of the solar wind Poynting flux is converted into ion outflow power when the ε parameter is around 10^{10} W. This value decreases to about 0.01% with increasing ε values. Contributions to ion outflow energization from solar illumination are about 6–7 orders of magnitude smaller than that of the solar wind electromagnetic energy input.

DISCUSSION

A recurring question concerning the escape of matter from planetary atmospheres is the role of an intrinsic planetary magnetic field [35,37]. For example, at Mars and Venus, the loss through atmospheric outflow has sometimes been attributed to the lack of an intrinsic magnetic field [99]. It has therefore somewhat naively been assumed that a strong planetary magnetic field and the presence of a magnetosphere prevent erosion of the atmosphere. However, this assumption was challenged when the cold ions were taken into account in estimations of total outflow rates. For example, the study by [40] concluded that previous estimates of ion outflow from Earth were underestimated. Updated values on outflow rates, where cold ions are included, suggests total outflow rates from Earth of the same order of magnitude as ion outflow rates from Mars reported in, e.g., Fränz et al. [100]; Persson et al. [101]; Ramstad and Barabash, (2021).

Different planets possess different atmospheres and have different energy transfer processes. In this context it is interesting to understand how the energy sources (solar EUV and solar wind energy) control the ion supply in the ionospheric source region and the energy needed to reach escape velocity and determine whether the outflow is limited by available ion sources or by energy available for the ions to reach escape velocity.

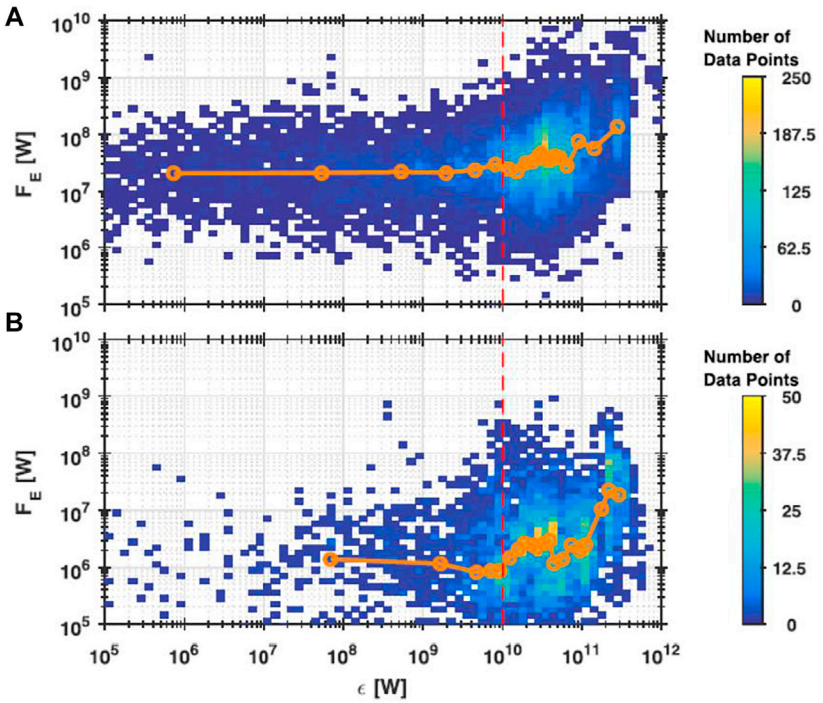

FIGURE 6 | Total hemispheric power, F_E, as a function of the ε parameter for the conditions where more than 95% of the polar cap is sunlit (**Figure 6A**) and dark (**Figure 6B**), respectively. Colored pixels show the numbers of data points in corresponding ranges of F_E and ε parameter. Values indicated by open circles are median values of F_E. Under conditions where ε is less than 10^{10} W, indicated by the red dash line, solar illumination is considered the main energy source of the cold ion outflow. From Li et al., (2018).

A simple model would include an ionospheric source of ions (ionization provided by solar EUV radiation; other ionization processes such as particle precipitation and cosmic ray absorption are ignored in this simple model) and energy for the ions to obtain escape velocity (energy carried by the solar wind, converted to suitable electromagnetic form to energize the ions). Reality is more complex, with both sources (solar EUV, solar wind) contributing to both the ionospheric source and the energy to reach escape velocity. As one can see in **Figure 5**, more solar EUV gives more ions (per unit area in the ionosphere). More solar EUV also gives higher ambipolar electric field and maybe slightly higher outflow velocity [76]. More solar wind energy gives higher ion density (higher scale height) in the ionosphere since some energy can be dissipated in the ionosphere and consequently higher ion outflow density (**Figure 5A**). More solar wind energy also gives larger polar cap area (**Figure 5E**). In **Figure 5B**, the ion outflow velocity does not really increase. The outflow flux increases since the density of the outflow increases, as comparing **Figure 5C** with **Figure 5A**. During geomagnetic storms also the velocity can increase but density is still more important for outflow per unit area [72]. The total outflow also increases with increased solar wind energy since the polar cap area increases (**Figure 5E**), which is the more important effect.

From the above analysis, the outflow mechanism can be said to be source-limited in the sense that increased outflow flux depends on higher density in the outflow than higher outflow speed. The cause may be increased solar EUV or solar wind energy through low-altitude energy deposition illustrated for another region for one geomagnetic storm in **Figure 1** of Strangeway et al. [11]). The outflow mechanism can also be said to be energy-limited in the sense that more solar wind energy will increase the outflow by increasing its density. The total outflow is energy-dependent also since the polar cap area is enlarged during periods of high solar wind energy input. Therefore, it is not simple to distinguish between source-limited or energy-limited in the case of ionospheric outflow from Earth, as that has been analyzed for Martian ionospheric outflow [37].

Other studies of ion outflow from Earth consider other regions and other ion species. One example is an investigation of the dayside high latitude region during a geomagnetic storm, dominated by O^+ ions [11,102]. In that study, two primary energy sources are considered; Poynting flux and soft electron precipitation, as observed by the FAST satellite at 4,000 km. The best controlling parameter is the density of precipitating electrons, but the energy sources are strongly correlated. The scenario is that the precipitating energy (originating in the solar wind) dissipated in the ionosphere increases the scale height and increases the number of upwelling ions. Note that not all of the precipitating energies could be traced back to the solar wind, one exception is the wave-induced electron precipitation (defined as the broadband precipitation by 110) originating from the ionosphere, although this type of precipitation mainly happens in the premidnight sector of aurora region. Wave energization is then needed to provide transverse (to the magnetic field) heating which, together with the magnetic mirror force in a converging/diverging geomagnetic field can cause ion outflow ([11], **Figure 1**). Here it is believed that increased (solar wind) energy input results in a higher ionospheric scale height (more ions in the source), while solar wind energy is needed for wave heating for the O^+ ions to reach escape

velocity. Since the [11] study is limited to a selected geomagnetic storm, seasonal and solar cycle effects such as varying solar EUV are not considered. They also point out that the results "should be used in conjunction with classical polar wind models".

It is also useful to compare the energy transfer efficiencies from our studies with investigations of ion outflow from other planets. Care must be taken when trying to reach general conclusions since the studies are obtained with different instruments, and cover different energies, ion masses and parts of the solar cycle. Recent estimates of the coupling coefficient by several researchers are based on different definitions, making it difficult to directly compare the energy transfer efficiencies [37,101]. Nevertheless, one interesting aspect is that an intrinsic planetary magnetic field has been considered as a "shield" needed for planets and exoplanets to protect the atmosphere and ionosphere. Recent simulations and estimates show that this assumption is not necessarily correct, an intrinsic field might well increase the outflow [35–37].

SUMMARY

Ionospheric outflow from the Earth mainly consists of cold ions with both kinetic and thermal energies smaller than 100 eV during geomagnetically quiet times. Cold ions are important to understand the ionospheric outflow, but measuring cold ions with regular ion detectors in space often suffers from spacecraft charging issue for a spacecraft operating in a sunlit and tenuous plasma environment. Statistical studies of cold ions in the polar lobes has not been available until the wake technique utilizing the electric field measurements from two complementary electric field instruments on Cluster satellites. The main conclusions from the wake method are summarized as below:

- The wake method has revealed and allowed characterization of cold ions previously invisible.
- Cold ions dominate the ion population in the magnetotail lobes and polar cap region, especially during geomagnetically quiet times.
- Average outflow rates are of the order of 10^{26} ions s^{-1}. One main source region of cold ions in the magnetosphere is the polar cap ionosphere with open magnetic field. During periods of geomagnetic storm, both the outflow flux and the size of polar cap increase.
- The fate of cold ions is controlled by the magnetospheric convection and the parallel velocities of cold ions. There are high fluxes of cold ions in the topside ionosphere during the geomagnetic storm periods. But because of high magnetospheric convection velocity, most of them could reach the plasma sheet before they are transported far in the magnetotail.
- Cold ion outflow is modulated by solar wind energy input and solar irradiation. About 0.01–0.1% of solar wind energy input is transferred to the cold ion outflow. While the efficiencies for solar irradiation transferring energy to cold ion outflow are 6–7 orders of magnitude smaller.
- Cold ion outflow is also affected by the orientation of the geomagnetic dipole axis. The orientation of the geomagnetic dipole axis controls the illuminated area of the polar cap and thus the outflow.
- Within the range of the magnetic field strength in the polar region of the southern hemisphere at present time, the strength of intrinsic magnetic field is anti-correlated with ionospheric outflow during the periods of high levels of solar activity.

For the outflow of cold ions in the polar cap and magnetotail lobes we investigate, solar EUV illumination and solar wind energy both contribute to the ionospheric source of ions and the energy needed to reach escape velocity. Usually, the increase of density rather than the increase of velocity is more important for the outflow per unit area when solar EUV illumination or solar wind energy is increased. In addition, the increase of the polar cap, the outflow area, with solar wind energy input, is an important factor for the total outflow.

Nevertheless, some fundamental question about the electric field enabling cold ions to escape remains to answer: how do the electrons from the polar rain and the photo-emission play a role in affecting the ambipolar electric field ? How is the ambipolar electric field affected by the solar wind and the geomagnetic condition? To answer these questions with observations, a special instrument proposed by Li et al. [103] should be built to measure the extremely small electric field.

It is still difficult to estimate from observations how much of the ionospheric ions in the plasma sheet will end up in various parts of the magnetosphere although some simulations have been conducted [104]. Many ions do not escape directly down the geomagnetic tail into the solar wind but return back to the magnetosphere [71] and some may be lost into the ionosphere [105], but most ions are likely to eventually leave the magnetosphere into the solar wind (e,g, André at al. 2015). Unlike O^+ ions, protons are heated and mixed up with ions of the solar wind. These protons of ionospheric origin become un-distinguishable from the solar wind, leading to a further complication to study the fate of the ionospheric ions.

AUTHOR CONTRIBUTIONS

KL, MA, SH, YW, and JC contributed to conception and design of the study. AE and MA organized the database. KL performed the statistical analysis. KL wrote the first draft of the manuscript. MA and SH wrote sections of the manuscript. All authors contributed to manuscript revision, read, and approved the submitted version.

FUNDING

This work was supported by the pre-research project on Civil Aerospace Technologies No. D020104 funded by China's National Space Administration, and the National Natural Science Foundation of China under Grant 41704164. MA is supported by the Swedish National Space Agency contract 2020-00058.

ACKNOWLEDGMENTS

MA and SH acknowledge support from the ISSI international team cold plasma of ionospheric origin at the Earth's

magnetosphere. We acknowledge the essential studies to measure cold ions with the wake method by E. Engwall. We also thank the tremendous help and contributions to the studies utilizing the cold ion data by L. Chai, P. W. Daly, M. Förster, M. Fränz, E. Grigorenko, E. Kronberg, L. Maes, R. Maggiolo, H. Nilsson, Q. Y. Ren, Z. J. Rong, W. X. Wan, and H. Zhao.

REFERENCES

1. Chappell CR, Baugher CR, and Horwitz JL. New Advances in thermal Plasma Research. *Rev Geophys* (1980) 18(4):853–61. doi:10.1029/RG018i004p00853
2. Chappell CR, Moore TE, and Waite JH. The Ionosphere as a Fully Adequate Source of Plasma for the Earth's Magnetosphere. *J Geophys Res* (1987) 92(A6):5896. doi:10.1029/JA092iA06p05896
3. Moore TE, Chappell CR, Chandler MO, Craven PD, Giles BL, Pollock CJ, et al. High-Altitude Observations of the Polar Wind *Science* (1997) 277(5324):349–51. doi:10.1126/science.277.5324.349
4. Olsen RC, Chappell CR, Gallagher DL, Green JL, and Gurnett DA. The Hidden Ion Population: Revisited. *J Geophys Res* (1985) 90(A12):12121–32. doi:10.1029/JA090iA12p12121
5. André M, Li K, and Eriksson AI. Outflow of Low-Energy Ions and the Solar Cycle. *J Geophys Res Space Phys* (2015) 120(2):1072–85. doi:10.1002/2014ja020714
6. Yamauchi M. Terrestrial Ion Escape and Relevant Circulation in Space. *Ann Geophys* (2019) 37:1197–222. doi:10.5194/angeo-37-1197-2019
7. Yau AW, Abe T, André M, Howarth AD, and Peterson WK. Ionospheric Ion Acceleration and Transport. In: R Maggiolo, N André, H Hasegawa, and DT Welling, editors. *Magnetospheres in the Solar System, Geophysical Monograph*. John Wiley & Sons (2021). doi:10.1002/9781119507512
8. André M, Eriksson AI, Khotyaintsev YV, and Toledo-Redondo S. The Spacecraft Wake: Interference with Electric Field Observations and a Possibility to Detect Cold Ions. *J Geophys Res Space Phys* (2021) 126: e2021JA029493. doi:10.1029/2021JA029493
9. Toledo-Redondo S, André M, Aunai N, Chappell CR, Dargent J, Fuselier SA, et al. Impacts of Ionospheric Ions on Magnetic Reconnection and Earth's Magnetosphere Dynamics. *Rev Geophys* (2021) 59:e2020RG000707. doi:10.1029/2020RG000707
10. André M, and Yau A. Theories and Observations of Ion Energization and Outflow in the High Latitude Magnetosphere. *Space Sci Rev* (1997) 80(1/2): 27–48. doi:10.1023/A:100492161988510.1007/978-94-009-0045-5_2
11. Strangeway RJ, Ergun RE, Su Y, Carlson CW, and Elphic RC. Factors Controlling Ionospheric Outflows as Observed at Intermediate Altitudes. *J Geophys Res* (2005) 110(A3). doi:10.1029/2004ja010829
12. Krcelic P, Haaland S, Maes L, Slapak R, and Schillings A. Estimating the Fate of Oxygen Ion Outflow from the High-Altitude Cusp. *Ann Geophys* (2020) 38(2):491–505. doi:10.5194/angeo-38-491-2020
13. Liao J, Kistler LM, Mouikis CG, Klecker B, Dandouras I, and Zhang J-C. Statistical Study of O+transport from the Cusp to the Lobes with Cluster CODIF Data. *J Geophys Res* (2010) 115(A12):a–n. doi:10.1029/2010ja015613
14. Schillings A, Slapak R, Nilsson H, Yamauchi M, Dandouras I, and Westerberg L-G. Earth Atmospheric Loss through the Plasma Mantle and its Dependence on Solar Wind Parameters. *Earth Planets Space* (2019) 71(1). doi:10.1186/s40623-019-1048-0
15. Seki K, Hirahara M, Terasawa T, Mukai T, Saito Y, Machida S, et al. Statistical Properties and Possible Supply Mechanisms of Tailward Cold O+beams in the Lobe/mantle Regions. *J Geophys Res* (1998) 103:4477–89. doi:10.1029/97ja02137
16. Slapak R, Nilsson H, and Westerberg LG. A Statistical Study on O+ Flux in the Dayside Magnetosheath. *Ann Geophys* (2013) 31:1005–10. doi:10.5194/angeo-31-1005-2013
17. Khazanov GV, Krivorutsky EN, and Sibeck DG. Formation of the Potential Jump over the Geomagnetically Quiet Sunlit Polar Cap Region. *J Geophys Res Space Phys* (2019) 124(6):4384–401. doi:10.1029/2019ja026576
18. Kitamura N, Seki K, Nishimura Y, Terada N, Ono T, Hori T, et al. Photoelectron Flows in the Polar Wind during Geomagnetically Quiet Periods. *J Geophys Res* (2012) 117(A7):a–n. doi:10.1029/2011ja017459
19. Axford WI. The Polar Wind and the Terrestrial Helium Budget. *J Geophys Res* (1968) 73:6855–9. doi:10.1029/JA073i021p06855
20. Banks PM, and Holzer TE. The Polar Wind. *J Geophys Res* (1968) 73(21): 6846–54. doi:10.1029/JA073i021p06846
21. Cladis JB, Collin HL, Lennartsson OW, Moore TE, Peterson WK, and Russell CT. Observations of Centrifugal Acceleration during Compression of Magnetosphere. *Geophys Res Lett* (2000) 27:915–8. doi:10.1029/1999GL010737
22. Comfort RH. The Magnetic Mirror Force in Plasma Fluid Models. In: TE Moore, JH Waite, TW Moorehead, and WB Hanson, editors. *Modeling Magnetospheric Plasma* (1988). p. 51–3. doi:10.1029/GM044p0051
23. Winglee RM, Chua D, Brittnacher M, Parks GK, and Lu G. Global Impact of Ionospheric Outflows on the Dynamics of the Magnetosphere and Cross-Polar Cap Potential. *J Geophys Res* (2002) 107(A9):1237. doi:10.1029/2001JA000214
24. Divin A, Khotyaintsev YV, Vaivads A, André M, Toledo-Redondo S, Markidis S, et al. Three-scale Structure of Diffusion Region in the Presence of Cold Ions. *J Geophys Res Space Phys* (2016) 121:001–12. doi:10.1002/2016JA023606
25. Toledo-Redondo S, André M, Khotyaintsev YV, Vaivads A, Walsh A, Li W, et al. Cold Ion Demagnetization Near the X-Line of Magnetic Reconnection. *Geophys Res Lett* (2016) 43(13):6759–67. doi:10.1002/2016gl069877
26. André M, Li W, Toledo-Redondo S, Khotyaintsev YV, Vaivads A, Graham DB, et al. Magnetic Reconnection and Modification of the Hall Physics Due to Cold Ions at the Magnetopause. *Geophys Res Lett* (2016) 43(13):6705–12. doi:10.1002/2016GL069665
27. Graham DB, Khotyaintsev YV, Norgren C, Vaivads A, André M, Toledo-Redondo S, et al. Lower Hybrid Waves in the Ion Diffusion and Magnetospheric Inflow Regions. *J Geophys Res Space Phys* (2017) 122: 517–33. doi:10.1002/2016JA023572
28. Steinvall K, Khotyaintsev YV, Graham DB, Vaivads A, André M, and Russell CT. Large Amplitude Electrostatic Proton Plasma Frequency Waves in the Magnetospheric Separatrix and Outflow Regions during Magnetic Reconnection. *Geophys Res Lett* (2021) 48:e2020GL090286. doi:10.1029/2020GL090286
29. Dargent J, Aunai N, Lavraud B, Toledo-Redondo S, and Califano F. Simulation of Plasmaspheric Plume Impact on Dayside Magnetic Reconnection. *Geophys Res Lett* (2020) 47:e2019GL086546. doi:10.1029/2019GL086546
30. Kulikov YN, Lammer H, Lichtenegger HIM, Penz T, Breuer D, Spohn T, et al. A Comparative Study of the Influence of the Active Young Sun on the Early Atmospheres of Earth, Venus, and Mars. *Space Sci Rev* (2007) 129(1-3): 207–43. doi:10.1007/s11214-007-9192-4
31. Lammer H, Zerkle AL, Gebauer S, Tosi N, Noack L, Scherf M, et al. Origin and Evolution of the Atmospheres of Early Venus, Earth and Mars. *Astron Astrophys Rev* (2018) 26(1):2. doi:10.1007/s00159-018-0108-y
32. Slapak R, Schillings A, Nilsson H, Yamauchi M, Westerberg L-G, and Dandouras I. Atmospheric Loss from the Dayside Open Polar Region and its Dependence on Geomagnetic Activity: Implications for Atmospheric Escape on Evolutionary Timescales. *Ann Geophys* (2017) 35:721–31. doi:10.5194/angeo-35-721-2017
33. Wei Y, Pu Z, Zong Q, Wan W, Ren Z, Fraenz M, et al. Oxygen Escape from the Earth during Geomagnetic Reversals: Implications to Mass Extinction. *Earth Planet Sci Lett* (2014) 394:94–8. doi:10.1016/j.epsl.2014.03.018
34. Wei Y, Fraenz M, Dubinin E, Woch J, Lühr H, Wan W, et al. Enhanced Atmospheric Oxygen Outflow on Earth and Mars Driven by a Corotating Interaction Region. *J Geophys Res* (2012) 117:a–n. doi:10.1029/2011JA017340
35. Gunell H, Maggiolo R, Nilsson H, Stenberg Wieser G, Slapak R, Lindkvist J, et al. Why an Intrinsic Magnetic Field Does Not Protect a Planet against Atmospheric Escape. *A&A* (2018) 614:L3. doi:10.1051/0004-6361/201832934
36. Gronoff G, Arras P, Baraka S, Bell JM, Cessateur G, Cohen O, et al. Atmospheric Escape Processes and Planetary Atmospheric Evolution. *J Geophys Res Space Phys* (2020) 125:e2019JA027639. doi:10.1029/2019JA027639

37. Ramstad R, and Barabash S. Do Intrinsic Magnetic Fields Protect Planetary Atmospheres from Stellar Winds?. *Space Sci Rev* (2021) 217. doi:10.1007/s11214-021-00791-1
38. Delzanno GL, Borovsky JE, Henderson MG, Resendiz Lira PA, Roytershteyn V, and Welling DT. The Impact of Cold Electrons and Cold Ions in Magnetospheric Physics. *J Atmos Solar-Terrestrial Phys* (2021) 220: 105599. doi:10.1016/j.jastp.2021.105599
39. Engwall E, Eriksson AI, and Forest J. Wake Formation behind Positively Charged Spacecraft in Flowing Tenuous Plasmas. *Phys Plasmas* (2006) 13(6): 062904. doi:10.1063/1.2199207
40. Engwall E, Eriksson AI, Cully CM, André M, Puhl-Quinn PA, Vaith H, et al. Survey of Cold Ionospheric Outflows in the Magnetotail. *Ann Geophys* (2009) 27:3185–201. doi:10.5194/angeo-27-3185-2009
41. Eriksson AI, André M, Klecker B, Laakso H, Lindqvist P-A, Mozer F, et al. Electric Field Measurements on Cluster: Comparing the Double-Probe and Electron Drift Techniques. *Ann Geophys* (2006) 24:275–89. doi:10.5194/angeo-24-275-2006
42. Svenes KR, Lybekk B, Pedersen A, and Haaland S. Cluster Observations of Near-Earth Magnetospheric Lobe Plasma Densities - a Statistical Study. *Ann Geophys* (2008) 26:2845–52. doi:10.5194/angeo-26-2845-2008
43. Grard RJL, and Jones D. An Evaluation of Experimental Errors in Electromagnetic Wave Measurements Aboard Satellites. *J Geophys Res* (1973) 78(25):5507–14. doi:10.1029/JA078i025p05507
44. Lybekk B, Pedersen A, Haaland S, Svenes K, Fazakerley AN, Masson A, et al. Solar Cycle Variations of the Cluster Spacecraft Potential and its Use for Electron Density Estimations. *J Geophys Res* (2012) 117(A1). doi:10.1029/2011ja016969
45. Trotignon JG, Décréau PME, Rauch JL, Randriamboarison O, Krasnoselskikh V, Canu P, et al. How to Determine the thermal Electron Density and the Magnetic Field Strength from the Cluster/Whisper Observations Around the Earth. *Ann Geophys* (2001) 19: 1711–20. doi:10.5194/angeo-19-1711-2001
46. Pedersen A, Lybekk B, André M, Eriksson A, Masson A, Mozer FS, et al. Electron Density Estimations Derived from Spacecraft Potential Measurements on Cluster in Tenuous Plasma Regions. *J Geophys Res* (2008) 113:a–n. doi:10.1029/2007JA012636
47. Gustafsson G, Boström R, Holback B, Holmgren G, Lundgren A, Stasiewicz K, et al. The Electric Field and Wave experiment for the Cluster mission. *Space Sci Rev* (1997) 79:137–56. doi:10.1023/A:1004975108657
48. Rème H, Aoustin C, Bosqued JM, Dandouras I, Lavraud B, Sauvaud JA, et al. First Multispacecraft Ion Measurements in and Near the Earth's Magnetosphere with Identical Cluster Ion Spectrometry (CIS) Experiments. *Ann Geophysicae* (2001) 19:1303–54. doi:10.5194/angeo-19-1303-2001
49. Johnstone AD, Alsop C, Burge S, Carter PJ, Coates AJ, Coker AJ, et al. Peace: A Plasma Electron and Current Experiment. *Space Sci Rev* (1997) 79:351–98. doi:10.1023/A:1004938001388
50. Décréau PME, Fergeau P, Fergeau P, Krannosels'Kikh V, Lévêque M, Martin P, et al. WHISPER, A Resonance Sounder and Wave Analyser: Performances and Perspectives for the Cluster Mission. *Space Sci Rev* (1997) 79:157–93. doi:10.1023/A:100493132640410.1007/978-94-011-5666-0_7
51. Haaland S, Svenes K, Lybekk B, and Pedersen A. A Survey of the Polar Cap Density Based on Cluster EFW Probe Measurements: Solar Wind and Solar Irradiation Dependence. *J Geophys Res* (2012) 117:A01216. doi:10.1029/2011JA017250
52. Haaland S, Lybekk B, Maes L, Laundal K, Pedersen A, Tenfjord P, et al. North-south Asymmetries in Cold Plasma Density in the Magnetotail Lobes: Cluster Observations. *J Geophys Res Space Phys* (2017) 122(1):136–49. doi:10.1002/2016ja023404
53. Engwall E, Eriksson AI, Cully CM, André M, Torbert R, and Vaith H. Earth's Ionospheric Outflow Dominated by Hidden Cold Plasma. *Nat Geosci* (2009) 2:24–7. doi:10.1038/ngeo387
54. Cully CM, Ergun RE, and Eriksson AI. Electrostatic Structure Around Spacecraft in Tenuous Plasmas. *J Geophys Res* (2007) 112:a–n. doi:10.1029/2007JA012269
55. Paschmann G, Quinn JM, Torbert RB, Vaith H, McIlwain CE, Haerendel G, et al. The Electron Drift Instrument on Cluster: Overview of First Results. *Ann Geophys* (2001) 19(10/12):1273–88. doi:10.5194/angeo-19-1273-2001
56. Paschmann G, Quinn JM, Torbert RB, McIlwain CE, Vaith H, Haaland S, et al. Results of the Electron Drift Instrument on Cluster. *J Geophys Res Space Phys* (2021) 126:e2021JA029313. doi:10.1029/2021JA029313
57. Hoffman JH, Dodson WH, Lippincott CR, and Hammack HD. Initial Ion Composition Results from the Isis 2 Satellite. *J Geophys Res* (1974) 79: 4246–51. doi:10.1029/JA079i028p04246
58. Shelley EG, Johnson RG, and Sharp RD. Satellite Observations of Energetic Heavy Ions during a Geomagnetic Storm. *J Geophys Res* (1972) 77:6104–10. doi:10.1029/JA077i031p06104
59. Yau AW, Peterson WK, and Abe T. Measurements of Ion Outflows from the Earth's Ionosphere. In: CR Chappell, RW Schunk, PM Banks, JL Burch, and RM Thorne, editors. 1st ed.. John Wiley & Sons (2017). p. 19–31. doi:10.1002/9781119066880.ch2*Geophys Monogr*
60. Yau AW, Abe T, and Peterson WK. The Polar Wind: Recent Observations. *J Atmos Solar-Terrestrial Phys* (2007) 69(16):1936–83. doi:10.1016/j.jastp.2007.08.010
61. Peterson WK, Andersson L, Callahan BC, Collin HL, Scudder JD, and Yau AW. Solar-minimum Quiet Time Ion Energization and Outflow in Dynamic Boundary Related Coordinates. *J Geophys Res* (2008) 113:a–n. doi:10.1029/2008JA013059
62. Torkar K, Riedler W, Escoubet CP, Fehringer M, Schmidt R, Grard RJL, et al. Active Spacecraft Potential Control for Cluster - Implementation and First Results. *Ann Geophys* (2001) 19:1289–302. doi:10.5194/angeo-19-1289-2001
63. Torkar K, Nakamura R, Tajmar M, Scharlemann C, Jeszenszky H, Laky G, et al. Active Spacecraft Potential Control Investigation. *Space Sci Rev* (2016) 199(1-4):515–44. doi:10.1007/s11214-014-0049-3
64. Su Y-J, Horwitz JL, Moore TE, Giles BL, Chandler MO, Craven PD, et al. Polar Wind Survey with the Thermal Ion Dynamics Experiment/Plasma Source Instrument Suite Aboard POLAR. *J Geophys Res* (1998) 103(A12): 29305–37. doi:10.1029/98JA02662
65. Peterson WK, Collin HL, Lennartsson OW, and Yau AW. Quiet Time Solar Illumination Effects on the Fluxes and Characteristic Energies of Ionospheric Outflow. *J Geophys Res* (2006) 111:A11S05. doi:10.1029/2005JA011596
66. Huddleston MM, Chappell CR, Delcourt DC, Moore TE, Giles BL, and Chandler MO. An Examination of the Process and Magnitude of Ionospheric Plasma Supply to the Magnetosphere. *J Geophys Res* (2005) 110:A12202. doi:10.1029/2004JA010401
67. Cully CM, Donovan EF, Yau AW, and Opgenoorth HJ. Supply of thermal Ionospheric Ions to the central Plasma Sheet. *J Geophys Res* (2003) 108(A2): 1092. doi:10.1029/2002JA009457
68. Yau AW, Howarth A, Peterson WK, and Abe T. Transport of thermal-energy Ionospheric Oxygen (O+) Ions between the Ionosphere and the Plasma Sheet and Ring Current at Quiet Times Preceding Magnetic Storms. *J Geophys Res* (2012) 117:a–n. doi:10.1029/2012JA017803
69. Li K, Haaland S, Eriksson A, André M, Engwall E, Wei Y, et al. On the Ionospheric Source Region of Cold Ion Outflow. *Geophys Res Lett* (2012) 39(18). doi:10.1029/2012gl053297
70. Li K, Haaland S, Eriksson A, André M, Engwall E, Wei Y, et al. Transport of Cold Ions from the Polar Ionosphere to the Plasma Sheet. *J Geophys Res Space Phys* (2013) 118(9):5467–77. doi:10.1002/jgra.50518
71. Haaland S, Eriksson A, Engwall E, Lybekk B, Nilsson H, Pedersen A, et al. Estimating the Capture and Loss of Cold Plasma from Ionospheric Outflow. *J Geophys Res* (2012) 117:a–n. doi:10.1029/2012JA017679
72. Haaland S, Eriksson A, André M, Maes L, Baddeley L, Barakat A, et al. Estimation of Cold Plasma Outflow during Geomagnetic Storms. *J Geophys Res Space Phys* (2015) 120(12). doi:10.1002/2015ja021810
73. Li K, Wei Y, André M, Eriksson A, Haaland S, Kronberg EA, et al. Cold Ion Outflow Modulated by the Solar Wind Energy Input and Tilt of the Geomagnetic Dipole. *J Geophys Res Space Phys* (2017) 122(10):658–10. doi:10.1002/2017ja024642
74. Li K, Wei Y, Haaland S, Kronberg EA, Rong ZJ, Maes L, et al. Estimating the Kinetic Energy Budget of the Polar Wind Outflow. *J Geophys Res Space Phys* (2018) 123(9):7917–29. doi:10.1029/2018ja025819
75. Li K, Förster M, Rong Z, Haaland S, Kronberg E, Cui J, et al. The Polar Wind Modulated by the Spatial Inhomogeneity of the Strength of the Earth's Magnetic Field. *J Geophys Res Space Phys* (2020) 125(4). doi:10.1029/2020ja027802

76. Maes L, Maggiolo R, De Keyser J, André M, Eriksson AI, Haaland S, et al. Solar Illumination Control of the Polar Wind. *J Geophys Res Space Phys* (2017) 122(11):11468–411480. doi:10.1002/2017ja024615
77. Northrop TG. *The Adiabatic Motion of Charged Particles*. New York: Interscience Publishers (1963).
78. Milan SE. Both solar Wind-Magnetosphere Coupling and Ring Current Intensity Control of the Size of the Auroral Oval. *Geophys Res Lett* (2009) 36(18). doi:10.1029/2009gl039997
79. Nilsson H, Waara M, Marghitu O, Yamauchi M, Lundin R, Rème H, et al. An Assessment of the Role of the Centrifugal Acceleration Mechanism in High Altitude Polar Cap Oxygen Ion Outflow. *Ann Geophys* (2008) 26:145–57. doi:10.5194/angeo-26-145-2008
80. Kistler LM. Ionospheric and Solar Wind Contributions to the Storm-Time Near-Earth Plasma Sheet. *Geophys Res Lett* (2020) 47:e2020GL090235. doi:10.1029/2020GL090235
81. Nilsson H, Engwall E, Eriksson A, Puhl-Quinn PA, and Arvelius S. Centrifugal Acceleration in the Magnetotail Lobes. *Ann Geophys* (2010) 28:569–76. doi:10.5194/angeo-28-569-2010
82. Nilsson H, Barghouthi IA, Slapak R, Eriksson AI, and André M. Hot and Cold Ion Outflow: Observations and Implications for Numerical Models. *J Geophys Res Space Phys* (2013) 118(1):105–17. doi:10.1029/2012ja017975
83. Pham KH, Lotko W, Varney RH, Zhang B, and Liu J. Thermospheric Impact on the Magnetosphere through Ionospheric Outflow. *J Geophys Res Space Phys* (2021) 126:e2020JA028656. doi:10.1029/2020JA028656
84. Weimer DR. Models of High-Latitude Electric Potentials Derived with a Least Error Fit of Spherical Harmonic Coefficients. *J Geophys Res* (1995) 100(A10): 19595–607. doi:10.1029/95JA01755
85. Haaland SE, Paschmann G, Förster M, Quinn JM, Torbert RB, McIlwain CE, et al. High-latitude Plasma Convection from Cluster EDI Measurements: Method and IMF-Dependence. *Ann Geophys* (2007) 25:239–53. doi:10.5194/angeo-25-239-2007
86. Glassmeier K-H, and Vogt J. Magnetic Polarity Transitions and Biospheric Effects. *Space Sci Rev* (2010) 155:387–410. doi:10.1007/s11214-010-9659-6
87. Cnossen I, and Richmond AD. How Changes in the Tilt Angle of the Geomagnetic Dipole Affect the Coupled Magnetosphere-Ionosphere-Thermosphere System. *J Geophys Res* (2012) 117:a–n. doi:10.1029/2012ja018056
88. Reshetnyak MY, and Pavlov VE. Evolution of the Dipole Geomagnetic Field. Observations and Models. *Geomagn Aeron* (2016) 56:110–24. doi:10.1134/S0016793215060122
89. Glocer A, Kitamura N, Toth G, and Gombosi T. Modeling Solar Zenith Angle Effects on the Polar Wind. *J Geophys Res* (2012) 117:a–n. doi:10.1029/2011ja017136
90. Kitamura N, Ogawa Y, Nishimura Y, Terada N, Ono T, Shinbori A, et al. Solar Zenith Angle Dependence of Plasma Density and Temperature in the Polar Cap Ionosphere and Low-Altitude Magnetosphere during Geomagnetically Quiet Periods at Solar Maximum. *J Geophys Res* (2011) 116(A8):a–n. doi:10.1029/2011ja016631
91. Perreault P, and Akasofu S-I. A Study of Geomagnetic Storms. *Geophys J Int* (1978) 54(3):547–73. doi:10.1111/j.1365-246X.1978.tb05494.x
92. Juárez MT, Tauxe L, Gee JS, and Pick T. The Intensity of the Earth's Magnetic Field over the Past 160 Million Years. *Nature* (1998) 394:878–81. doi:10.1038/29746
93. Cole KD. Airglow and the South Atlantic Geomagnetic Anomaly. *J Geophys Res* (1961) 66(9):3064. doi:10.1029/JZ066i009p03064
94. Finlay CC, Kloss C, Olsen N, Hammer MD, Tøffner-Clausen L, Grayver A, et al. The CHAOS-7 Geomagnetic Field Model and Observed Changes in the South Atlantic Anomaly. *Earth Planets Space* (2020) 72:156. doi:10.1186/s40623-020-01252-9
95. Abdu MA, Batista IS, Carrasco AJ, and Brum CGM. South atlantic Magnetic Anomaly Ionization: A Review and a New Focus on Electrodynamic Effects in the Equatorial Ionosphere. *J Atmos Solar-Terrestrial Phys* (2005) 67(17-18): 1643–57. doi:10.1016/j.jastp.2005.01.014
96. Koch S, and Kuvshinov A. Does the South Atlantic Anomaly Influence the Ionospheric Sq Current System? Inferences from Analysis of Ground-Based Magnetic Data. *Earth, Planets and Space* (2015) 67:10. doi:10.1186/s40623-014-0172-0
97. Laundal KM, Cnossen I, Milan SE, Haaland SE, Coxon J, Pedatella NM, et al. North-south Asymmetries in Earth's Magnetic Field. *Space Sci Rev* (2017) 206:225–57. doi:10.1007/s11214-016-0273-0
98. Kopp G, and Lean JL. A New, Lower Value of Total Solar Irradiance: Evidence and Climate Significance. *Geophys Res Lett* (2011) 38:a–n. doi:10.1029/2010GL045777
99. Jakosky BM, Slipski M, Benna M, Mahaffy P, Elrod M, Yelle R, et al. Mars' Atmospheric History Derived from Upper-Atmosphere Measurements of38Ar/36Ar. *Science* (2017) 355(6332):1408–10. doi:10.1126/science.aai7721
100. Fränz M, Dubinin E, Nielsen E, Woch J, Barabash S, Lundin R, et al. Transterminator Ion Flow in the Martian Ionosphere. *Planet Space Sci* (2010) 58(11):1442–54. doi:10.1016/j.pss.2010.06.009
101. Persson M, Futaana Y, Ramstad R, Schillings A, Masunaga K, Nilsson H, et al. Global Venus-Solar Wind Coupling and Oxygen Ion Escape. *Geophys Res Lett* (2021) 48(3). doi:10.1029/2020gl091213
102. Tsyganenko NA. Modeling the Dynamics of the Inner Magnetosphere during strong Geomagnetic Storms. *J Geophys Res* (2005) 110(A3). doi:10.1029/2004ja010798
103. Li K, Haaland S, and Wei Y. A New Concept to Measure the Ambipolar Electric Field Driving Ionospheric Outflow. *J Geophys Res Space Phys* (2021) 126(2). doi:10.1029/2020ja028409
104. Moore TE, Fok M-C, and Garcia-Sage K. The Ionospheric Outflow Feedback Loop. *J Atmos Solar-Terrestrial Phys* (2014) 115-116:59–66. doi:10.1016/j.jastp.2014.02.002
105. Seki K, Elphic RC, Hirahara M, Terasawa T, and Mukai T. On Atmospheric Loss of Oxygen Ions from Earth through Magnetospheric Processes. *Science* (2001) 291(5510):1939–41. doi:10.1126/science.1058913
106. André M., and Cully C. M. (2012). Low-Energy ions: A Previously Hidden Solar System Particle Population. *Geophys Res Lett* 39:L03101. doi:10.1029/2011GL050242
107. Welling D. T., André M., Dandouras I., Delcourt D., Fazakerley A., Fontaine D., et al. (2015) The Earth: Plasma Sources, Losses, and Transport Process *Space Sci Rev* 192:145–208. doi:10.1007/s11214-015-0187-2
108. Vernov S. N., Gorchakov E. V., Shavin P. I., and Sharvina K. N.Radiation Belts in the Region of the South-Atlantic Magnetic Anomaly. *Space Sci Rev* (1967) 7:490–533. doi:10.1007/BF00182684
109. Jacobs J. A.Variations in the Intensity of the Earth's Magnetic Field. *Surveys Geophys* (1998) 19:139–187. doi:10.1023/A:1006579708430
110. Newell P. T., Liou K., and Wilson G. R.Polar Cap Particle Precipitation and Aurora: Review and Commentary. *J Atmos Solar-Terr Phys* (2009) 71: 199–215. doi:10.1016/j.jastp.2008.11.004

Conflict of Interest: The authors declare that the research was conducted in the absence of any commercial or financial relationships that could be construed as a potential conflict of interest.